Vol. 13, No. 2, 2022
ISSN 2233-4203/ e-ISSN 2093-8950
ARTICLE www.msletters.org | Mass Spectrometry Letters

Lipid *N*-formylation Occurs During Fixation with Formalin

Min Jung Kim[1†], Heejin Lim[2†], Muwoong Kim[3], Yuri Choi[1], Thy N. C. Nguyen[2], Seung Cheol Park[1], Kwang Pyo Kim[1], Junyang Jung[3], and Min-Sik Kim[2]*

[1]*Department of Applied Chemistry, College of Applied Science, Kyung Hee University, Yongin-si, Gyeonggi-do 17104, Korea*
[2]*Department of New Biology, Daegu Gyeongbuk Institute of Science and Technology (DGIST), Daegu 42988, Korea.*
[3]*Department of Anatomy and Neurobiology, College of Medicine, Kyung Hee University, Seoul 02447, Korea*

Received March 31, 2022, Revised April 17, 2022, Accepted April 19, 2022
First published on the web June 30, 2022; DOI: 10.5478/MSL.2022.13.2.35

Abstract : Human tissues and organs can be preserved intact by fixation with formalin for the future analysis of biomolecules of interest. With the advances in high-throughput methods, numerous protocols have been developed and optimized to attain the most pathophysiological information out of biomolecules, including RNA and proteins, in formalin-fixed samples. However, there is no systematic study to examine the effects of formalin fixation on the lipidome of biological samples in a global fashion. In this study, we conducted a mass spectrometry-based analysis to survey the alteration in the lipidome of mice brains by fixation methods. A total of 308 lipids were quantitatively measured using triple quadrupole mass spectrometry. We found that most were unchanged after formalin fixation except for a few lipid classes such as phosphatidylethanolamine.

Keywords : formalin fixation, *N*-formylation, mass spectrometry-based lipidomics

Introduction

Patient-derived clinical samples are generally preserved by fixation for long-term storage and future usage.[1] A tremendous number of clinical samples have been stored by this method, along with patient-associated meta-information. Tissue microarray using fixative-embedded patient samples is one of the foremost techniques for histological analysis in the last decade.[2] Recent advances in high-throughput technologies, namely RNA-Seq and mass spectrometry-based proteomics, allow one to analyze biomolecules in fixed tissues.[3-7] Besides alcoholic-based fixatives, formaldehyde (or so-called formalin) is among the most commonly used fixatives due to its advantages.[8,9]

Yet, this chemical reagent reacts with biomolecules, forming intramolecular and intermolecular cross-linked species.[10] Cross-linking occurs with lysine, arginine, tyrosine, asparagine, and glutamine[10] residues of proteins, which can hinder their enzyme activities.

Since several amino acids are known to be modified by formaldehyde, similar reactions may occur with lipids.[10] However, there is no systematic study on the effects of formalin fixation on lipid extraction protocol for the lipidomic analysis. Lipids are mostly classified based on their chemical backbone structures.[11] Each lipid class and compounds play an important biological role in the cellular system, particularly energy storage, cell signaling,[12] and foundation of cell membrane's structure.[13-16] Here, we employed triple-quadrupole mass spectrometry-based lipidome profiling method to assess the global effect of this fixative on lipids. We have screened 308 lipids from mice samples by carrying out liquid chromatography-multiple reaction monitoring (LC-MRM) experiments. As a result, we found that the most of lipids analyzed in this study remained unchanged, while phosphatidylethanolamine (PtdEtn), lysophosphatidylethanolamine (lysoPtdEtn), cholesteryl ester (CE), and lysophosphatidylserine (lysoPtdSer) were altered in their abundance upon the fixation with formaldehyde.

Experimental

Materials and reagents

HPLC-grade acetonitrile, methanol, water, 2-propanol, chloroform were purchased from J.T. Baker (Avantor Performance Material, Inc., Center Valley, PA, USA). Fluka Analytical HPLC-grade formic acid, hydrochloric

†These authors contributed equally.
*Reprint requests to Min-Sik Kim
https://orcid.org/0000-0001-7317-5360
E-mail: mkim@dgist.ac.kr

acid, ammonium formate, and acetic acid were purchased from Sigma-Aldrich. Lipid standards used in this study such as cholesteryl ester (CE) (10:0), monoacylglycerols (MAG) (15:1), diacylglycerols (DAG) (8:0-8:0), and triacylglycerol (TAG) (11:1-11:1-11:1) were purchased from Larodan Fine Chemicals AB (Malmö, Sweden). Phosphatidylcholine (PtdCho) (10:0-10:0), phosphatidylethanolamine (PtdEtn) (10:0-10:0), phosphatidylglycerol (PtdGro) (10:0-10:0), phosphatidylinositol (PtdIns) (8:0-8:0), phosphatidylserine (PtdSer) (10:0-10:0), phosphatidic acid (PtdOH) (10:0-10:0), lysophosphatidylcholine (lysoPtdCho) (13:0), lysophosphatidylethanolamine (lysoPtdEtn) (13:0), lysophosphatidylglycerol (lysoPtdGro) (14:0), lysophosphatidylinositol (lysoPtdIns) (13:0), lysophosphatidylserine (lysoPtdSer) (17:1), lysophosphatidic acid (lysoPtdOH) (17:0), sphingomyelin (CerPCho) (d18:1-12:0), ceramide (Cer) (d18:1-12:0), dihydroceramide (dhCer) (d18:0-12:0), sphingosine (Sph) (17:1), sphinganine (SPA) (17:0), ceramide-1-phosphate (C1P) (d18:1-12:0), dihydroceramide-1-phosphate (dhC1P) (d18:0-16:0), sphingosine-1-phosphate (S1P) (17:1), and sphinganine-1-phosphate (SPA1P) (C17:0) were purchased from Avanti Polar Lipids, Inc. (Alabaster, AL, USA).

Sample preparation

Five-week-old male C57BL/6 mice were obtained from Daehan Biolink (Gyeonggi-do, Republic of Korea). All animal procedures and sacrifices were performed in accordance with the guidelines of the Korean Academy of Medical Science and the approval of the Kyung Hee University Committee of Animal Research (approval number: KHUASP[SE]-16-043). Each mouse was sacrificed by CO_2 asphyxiation. Subsequently, the fresh brains were dissected from mice, immediately progressed to lipid extraction, and the fixation tissue was maintained in 4% paraformaldehyde (PFA) for fixation at 4°C for 5 days. Then the tissue was placed in water for a rinse.

Lipid extraction

Each lipid standard was dissolved in chloroform/methanol (1:1, v/v) and stored at -20°C and it was diluted to the desired concentration for extraction. To extract more anionic lipids, two-step extraction method that can disrupt ionic interactions between acidic lipids and proteins was used for extraction. Firstly, the extracted brain was added to 1 mL of chloroform/methanol (1:2, v/v) with 1 μg/mL solution of the commercial lipids mentioned above as internal standards. The samples were homogenized using a hand-type homogenizer and sonicated for 1 min. The samples were vortexed 3 × 30 s and incubated at room temperature for 10 min. After centrifugation (13,800 × g, 2 min at 4°C), 950 μL of supernatant was transferred to a new 1.5 mL tube. Secondly, the remaining pellet was dissolved in 750 μL of chloroform/methanol/37% HCl (40:80:1, v/v/v) and incubated for 15 min at room temperature with vortexing 3 × 30 s. Then, 250 μL of cold chloroform and 450 μL of cold 0.1 N HCl were added to the sample. Next, the samples were vortexed for 1 min and centrifuged (6,500 × g, 2 min at 4°C). The bottom organic phase was collected and pooled with a prior extract. Subsequently, the samples were equally divided into two aliquots and dried by a SpeedVac concentrator. One of the dried samples was then dissolved in 200 μL of solvent A/solvent B (2:1, v/v) for neutral and positive lipid analysis, and the other sample was dissolved in 200 μL of methanol for the trimethylsilyldiazomethane (TMSD) methylation reaction to analyze anionic lipids.

TMSD methylation

It is difficult to analyze acidic lipids by LC-MS due to peak tailing. So, we used a TMSD methylation method.[17] A 2 M solution of TMSD in hexane was added to the lipid extracts dissolved in methanol, and then the color of the solution was changed to yellow. After vortexing for 30 s, methylation was performed at 37°C for 15 min. Glacial acetic acid was added to quench the reaction of methylation for subsequent analysis. The samples were then subjected to LC-MS analysis.

Global lipid analysis of brain samples by using HPLC-MS

The HPLC analysis was performed on an Agilent 1290 infinity series HPLC instrument (Agilent Technologies, Santa Clara, CA, USA) equipped with a binary pump (G20A), an autosampler (G4226A), a column compartment (G1316C), and a thermostat (G1330B). Hypersil GOLD column (2.1 × 100 mm ID; 1.9 μm, Thermo Fisher Scientific, Waltham, MA, USA) was used for the separation of lipids. The temperatures of the sample tray and column oven were adjusted to 4°C and 40°C, respectively. Solvent A consisted of methanol-acetonitrile-water (19:19:2) with 20 mM ammonium formate and 0.1% (v/v) formic acid, and solvent B consisted of 2-propanol with 20 mM ammonium formate and 0.1% (v/v) formic acid. The flow rate was 0.25 mL/min and the injection volume was 4 μL for each run. A 33 min gradient was performed as follows: 0-5 min, B 5%; 5-15 min, B 30%; 15-22 min, B 90% and maintained for 5 min. Finally, the column was equilibrated at B 5% for 5 min before reuse. Lipid analysis of brain tissue was performed by a triple quadrupole mass spectrometer (QQQ LC-MS 6490 series, Agilent Technologies). The parameters of operating source conditions were as follows: capillary voltage 4,000 V and nozzle voltage 500 V. The gas flow rate and nebulizer gas flow rate were set to 13 L/min and 40 psi. All lipids were analyzed under optimized conditions in MRM mode using computed transitions for each lipid class.

Data processing of individual data obtained by MRM

Agilent Mass Hunter Workstation Data Acquisition software was used to process LC-MS data. Qualitative

Analysis B.06.00 software (Agilent Technologies, Wilmington, DE, USA) was used to export the m/z of precursor ions, product ions, and retention time. Lipid peaks could be assigned by comparing to the retention time of each lipid class internal standard because lipids are separated based on their fatty acid compositions.[18] The MRM data of each assigned lipid from the replicated experiment was calculated for the assigned lipid's peak area by using Skyline software package (MacCoss Laboratory, University of Washington, Seattle, WA, USA).

MALDI-TOF experiment of PtdEtn modified with formalin

A total amount of 10 μg of phosphatidylethanolamine was incubated with or without 4% formalin at 4°C in dark overnight. The phosphatidylethanolamine samples were desalted with C18 column and then mixed with binary matrix solution (7 mg each of 2, 5-dihydroxybenzoic acid (DHB) and α-cyano-4-hydroxycinnamic acid (HCCA) in 1 mL of 0.1% TFA in 70% methanol).[19] Next, a total of 1.5 μL of samples were spotted onto a 384-target plate (BrukerDaltonics, Bremen, Germany) and dried in the desiccator for homogeneous matrix crystallization. MALDI-MS analysis was performed by an UltrafleXtreme mass spectrometer equipped with a 200 Hz Smartbeam laser as an ionization source on positive mode. All mass spectra were acquired with a set of parameters (delay time, 180 ns; ion source 1 voltage, 25 kV; ion source 2 voltage, 21.65 kV; and lens voltage, 9.2 kV). The detection range of MALDI-TOF mass spectrometry analysis was between 500 Da and 1,200 Da and an average of 1000 shots/spot was acquired. External calibration was carried out using the PtdEtn standard whenever MS data are acquired.

Results and Discussion

Freezing does not affect lipidomes of brains

To minimize a variation among the samples, mice brains were dissected in less than half an hour of sacrifice and quickly homogenized by a hand-type homogenizer to extract lipidomes from either fresh, frozen, or formalin-fixed brains in the presence of lipid standards, as shown in Figure 1. One of the problems of the lipidomic pipeline is the peak tailing of acidic lipids, such as phosphatidic acid (PtdOH), phosphatidylinositol (PtdIns), phosphatidylserine (PtdSer), lysophosphatidic acid (lysoPtdOH), lysophosphatidylinositol (lysoPtdIns), lysophosphatidylserine (lysoPtdSer), and ceramide-1-phosphate (C1P), making it difficult to achieve quantitative liquid chromatography analysis. So, we applied the relatively rapid and simple derivatization method by methylation to the phosphate group to reduce the peak tailing as previously shown.[17,20] Then we carried out a comparative lipidomic analysis between the fresh and frozen brains to justify the effects of the snap-freezing process and subsequent storage into the deep freezer on lipidomic analysis. Supplementary Table S1 shows the full list of transitions associated with lipids analyzed that were monitored, and Table 1 summarized the numbers of transitions monitored and lipids observed in this study. For example, 32 lipids were measured among 93 lipids within the phosphatidylethanolamine (PtdEtn) lipid class.

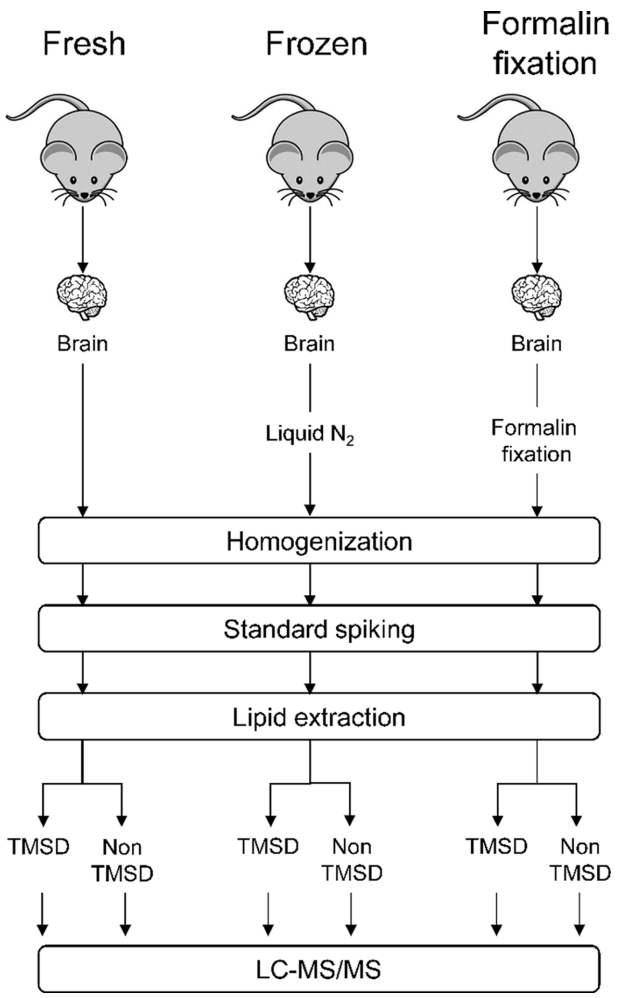

Figure 1. Overall workflow for mining differently regulated lipids (DRLs). Mouse brains were prepared fresh, frozen, or formalin-fixed. Lipids were extracted from the intact brain samples by homogenization along with lipid standards. A part of lipids was modified with TMSD while the other part was unmodified for the LC-MS/MS analysis. Samples were analyzed in quintuplicate.

The purpose of this study is to see if the lipids extracted from tissues stored at the different statuses (*e.g.* fresh, frozen, or formalin-fixed) show any change in their abundance. Thus, we compared the abundance of these observed lipids between different experiments. As shown in Figure 2A, there was no significant change in the abundance of lipids screened between fresh and frozen brains. This result indicates that the freezing process does not affect lipids significantly.

Table 1. Lipid classes and their numbers of lipid transitions detected.

The number of detected lipid transitions / All transitions			
Class	Detected	Class	Detected
CE	12/23	dhCer	6/69
Cholesterol	1/1	PtdGro	4/93
MAG	5/23	lysoPtdGro	5/22
DAG	9/93	PtdOH	6/93
TAG	35/194	lysoPtdOH	16/23
PtdCho	44/93	PtdIns	7/93
lysoPtdCho	18/23	lysoPtdIns	5/23
PtdEtn	32/93	PtdSer	32/93
lysoPtdEtn	18/22	lysoPtdSer	11/23
Sph	1/3	C1P	10/68
Cer	12/69	SPA1P	0/3
CerPCho	14/23	S1P	0/3
SPA	0/3	dhCer1P	0/67

Formalin fixation does affect lipidomes of brains

Next, we compared the abundances of lipids detected in common between fresh and formalin-fixed brains, resulting in 308 overlapping lipids as shown in Figure 3A. To see if there is a bias in the abundance of a lipid class, we plotted the volcano plot of the fold-change versus the p-values of lipids observed in common between fresh and formalin-fixed brains (Figure 3B). Interestingly, only a few lipid classes were found to be affected by the fixation with formalin while most of the lipids remained unchanged. Notably, CE and lysoPtdSer classes of lipids were increased in their extraction while PtdEtn class was decreased in their abundance with formalin fixation. A total of 32 altered lipids belong to PtdEtn, suggesting the impact of formalin on this specific class of lipids. Table 2 shows that the abundance of representative PtdEtn lipid molecules decreased by the fixation with formalin.

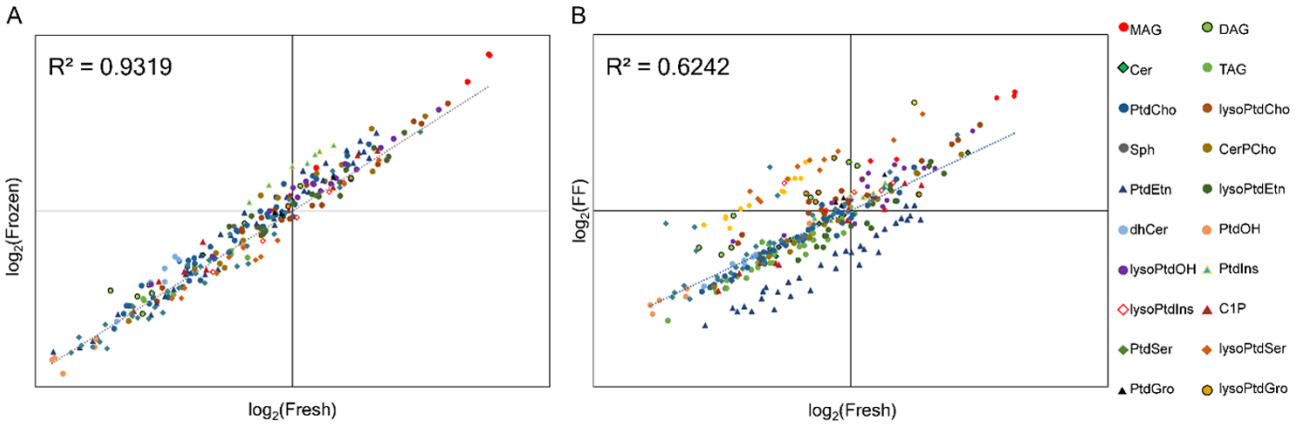

Figure 2. Relative abundance of lipidome. A total of 20 different lipid classes were observed in this analysis. The area under the liquid chromatographic curve was estimated to represent the abundance of each lipid. (A) Scatter plot of $\log_2$ (abundance) of lipids between fresh and frozen brains with R^2 of 0.9319. (B) Scatter plot of $\log_2$ (abundance) of lipids between fresh and formalin-fixed brains is shown along with R^2 of 0.6242.

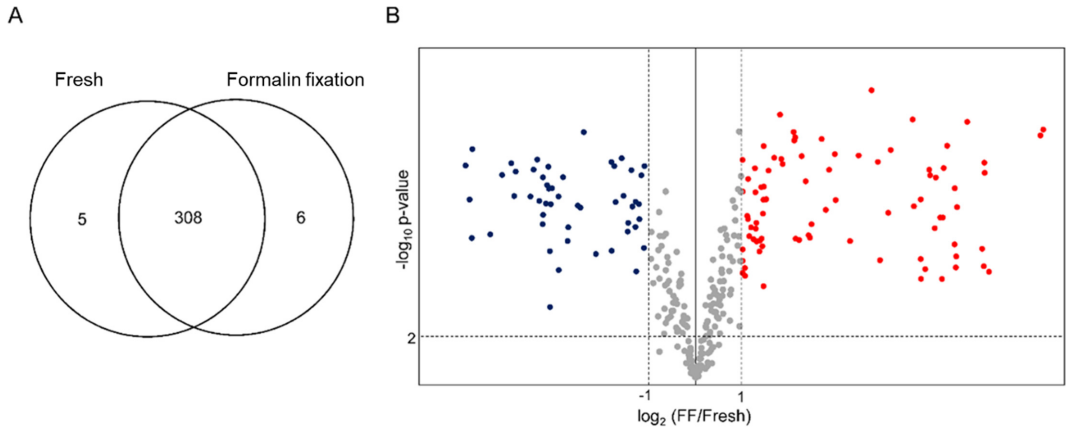

Figure 3. Altered lipids by fixation. (A) Venn diagram shows lipids detected from fresh and formalin-fixed brains. A total of 308 lipids were observed in common. (B) Volcano plot shows altered lipids by fixation when compared to fresh lipids (p-value < 0.01, fold change ≥ 2).

Table 2. Top 10% of over, less represented lipids in formalin fixed brain (p-value < 0.01, Fold change > 2).

Over represented lipids in formalin fixed brain					Less represented lipids in formalin fixed brain				
Species	Precursor ion	Product ion	P-value	Ratio *	Species	Precursor ion	Product ion	P-value	Ratio *
PS(32:1) **	762.6	549.3	4.94×10^{-11}	185.87	PE(38:2)	772.4	631.3	1.53×10^{-9}	0.03
PS(38:4) **	840.6	627.3	8.72×10^{-11}	177.95	PE(40:2)	800.4	659.3	3.97×10^{-8}	0.03
LPS(16:1) **	524.3	311.2	3.94×10^{-5}	82.18	PE(42:1)	830.4	689.3	1.58×10^{-6}	0.03
ChE(20:4)	690.6	369.2	3.06×10^{-9}	77.06	PE(38:1)	774.4	633.3	3.20×10^{-10}	0.03
Cholesterol	404	369.2	1.18×10^{-9}	76.62	PE(40:1)	802.4	661.3	1.11×10^{-6}	0.05
LPS(22:1) **	608.3	395.2	2.32×10^{-5}	76.16					
LPS(20:0) **	582.3	369.2	4.37×10^{-6}	74.23					
PS(38:2) **	844.6	631.3	2.37×10^{-11}	59.31					

* Ratio, formalin fixed brain/fresh brain

** Anionic lipids analyzed after TMSD derivatization

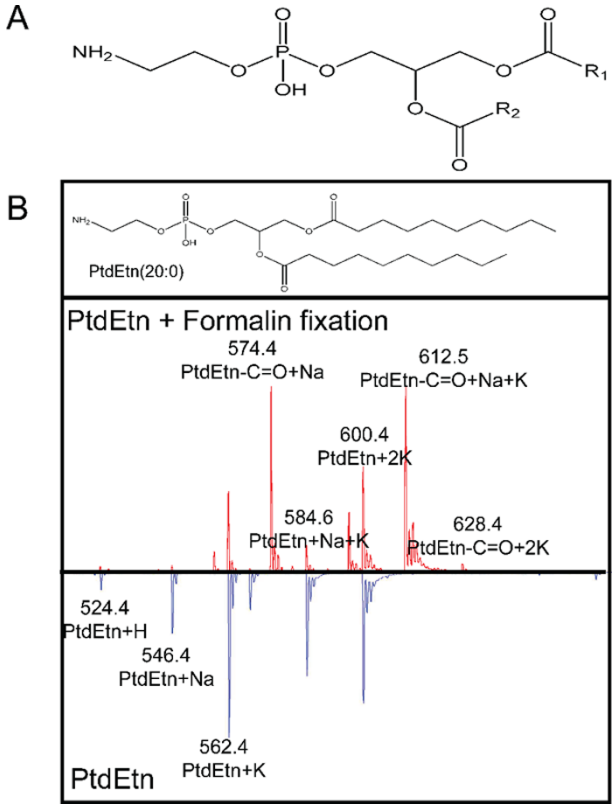

Figure 4. Modification of PtdEtn by formalin. (A) Molecular structure of PtdEtn has a primary amine group. (B) MALDI spectra of PtdEtn (20:0) and formalin-modified PtdEtn (20:0) with spectral annotation.

N-formylation occurs by formalin

Proteins are modified with formalin,[1] which usually occurs on the primary amine functional group (e.g. N-terminus and/or lysine side chain). Interestingly, one major class of altered lipids observed during the formalin fixation was PtdEtn, which contains primary amine on their structure (Figure 4A). PtdEtn is a glycerophospholipid, in which a PtdEtn moiety occupies a glycerol substitution site in addition to primary amine functional group. It can also have many different combinations of fatty acids of varying lengths and saturation attached to the C-1 and C-2 positions. For example, PtdEtn (10:0/10:0), also known as PtdEtn (20:0), consists of two decanoyl chains at positions C-1 and C-2 as shown in the inset of Figure 4B. To substantiate the modification of PtdEtn by formalin, we analyzed formalin-fixed PtdEtn (20:0) by MALDI-TOF MS analysis. As shown in the standard PtdEtn spectrum (20:0) (Figure 4B), a few major peaks were observed as adduct forms with hydrogen, sodium, and potassium (m/z 524, 546, and 562, respectively). Whereas, several peaks, on the top spectrum, were found to be shifted at higher masses that indicated N-formylation modification induced by formalin. As seen in Figure 4B, all the shifted masses are exactly associated with the mass of carbonyl group of formalin (-CO, m/z = 28) as annotated.

Conclusion

Lipids in cells are one of the important classes of biomolecules and they represent cell status. Thus, many studies have been performed to monitor lipids in biomedical research. Recent advances in sequencing technologies allow researchers to study biomolecules in a high-throughput fashion on a set of collected samples. In general, tissues are preserved by fixation with formalin for future analysis. Here we systematically analyzed the global lipids using ESI-LC-MS to investigate the lipid classes that could be altered during the fixation process. We found no significant alteration in samples with the freezing method, yet a slight change by formalin fixation. In total, 308 lipids were quantitatively profiled using an Agilent triple quadrupole mass spectrometer, of which some lipid classes were altered, including PtdEtn. The PtdEtn lipid class contains a

primary amine functional group, similar to the side chain of lysine amino acid on proteins that were known to be modified by formalin. To confirm this type of modification on PtdEtn by formalin, we further carried out MALDI-TOF MS analysis for formalin-fixed PtdEtn (20:0). We found that all mass shifts were equivalent to the mass of the carbonyl group of formalin, indicating N-formylation. In conclusion, most lipids remained unaffected by the fixation while a few molecules in PtdEtn, lysoPtdSer, and CE classes were altered. Nonetheless, further studies are required to evaluate the increase of lipids after fixation for a comprehensive understanding of this concern, in order to establish the optimal procedure for tissue preservation.

Acknowledgments

This study was supported by a grant from Kyung Hee University in 2016 (KHU-20161378) and a grant by the Brain Research Program through the National Research Foundation (NRF) funded by the Ministry of Science and ICT (MSIT) (Grant number: NRF-2017M3C7A1027472).

References

1. Gustafsson, O. J.; Arentz, G.; Hoffmann, P. *Biochim. Biophys. Acta.* **2015**, 1854, 559, DOI: 10.1016/j.bbapap.2014.10.003.
2. Kallioniemi, O. P.; Wagner, U.; Kononen, J.; Sauter, G. *Hum. Mol. Genet.* **2001**, 10, 657, DOI: 10.1093/hmg/10.7.657.
3. Wojakowska, A.; Marczak, L.; Jelonek, K.; Polanski, K.; Widlak, P.; Pietrowska, M. *PLoS One* **2015**, 10, e0136902, DOI: 10.1371/journal.pone.0136902.
4. Kokkat, T. J.; Patel, M. S.; McGarvey, D.; LiVolsi, V. A.; Baloch, Z. W. *Biopreserv Biobank* **2013**, 11, 101, DOI: 10.1089/bio.2012.0052.
5. Morton, M. L.; Bai, X.; Merry C. R.; Linden, A. L; Khalil, A. M.; Leidner, R. S.; Thompson, C. L. *Lung cancer* **2014**, 85, 1, DOI: 10.1016/j.lungcan.2014.03.020.
6. Steiner, C.; Tille, J.-C.; Lamerz, J.; Geijtenbeek, S. K. V.; McKee, T. A.; Venturi, M.; Rubbia-Brandt, L.; Hochstrasser, D.; Cutler, P.; Lescuyer, P.; Ducret, A. *Mol. Cell. Proteom.* **2015**, 14, 2786, DOI: 10.1074/mcp.O115.049049.
7. Moran, S.; Vizoso, M.; Martinez-Cardus, A.; Gomez, A.; Matias-Guiu, X.; Chiavenna, S. M.; Fernandez, A. G.; Esteller, M. *Epigenetics* **2014**, 9, 829, DOI: 10.4161/epi.28790.
8. Buesa, R. *J. Ann. Diagn. Pathol.* **2008**, 12, 387, DOI: 10.1016/j.anndiagpath.2008.07.004.
9. Werner, M.; Chott, A.; Fabiano, A.; Battifora, H. *Am. J. Surg. Pathol.* **2000**, 24, 1016, DOI: 10.1097/00000478-200007000-00014.
10. Hoffman, E. A.; Frey, B. L.; Smith, L. M.; Auble, D. T. *J. Biol. Chem.* **2015**, 290, 26404, DOI: 10.1074/jbc.R115.651679.
11. Fahy, E.; Subramaniam, S.; Brown, H. A.; Glass, C. K.; Merrill, A. H., Jr.; Murphy, R. C.; Raetz, C. R.; Russell, D. W.; Seyama, Y.; Shaw, W.; Shimizu, T.; Spener, F.; van Meer, G.; VanNieuwenhze, M. S.; White, S. H.; Witztum, J. L.; Dennis, E. A. *J. Lipid Res.* **2005**, 46, 839, DOI: 10.1194/jlr.E400004-JLR200.
12. Wenk, M. R. *Nat. Rev. Drug Discov.* **2005**, 4, 594, DOI: 10.1038/nrd1776.
13. Dennis, E. A.; Deems, R. A.; Harkewicz, R.; Quehenberger, O.; Brown, H. A.; Milne, S. B.; Myers, D. S.; Glass, C. K.; Hardiman, G.; Reichart, D.; Merrill, A. H., Jr.; Sullards, M. C.; Wang, E.; Murphy, R. C.; Raetz, C. R.; Garrett, T. A.; Guan, Z.; Ryan, A. C.; Russell, D. W.; McDonald, J. G.; Thompson, B. M.; Shaw, W. A.; Sud, M.; Zhao, Y.; Gupta, S.; Maurya, M. R.; Fahy, E.; Subramaniam, S. *J. Biol. Chem.* **2010**, 285, 39976, DOI: 10.1074/jbc.M110.182915.
14. Subramaniam, S.; Fahy, E.; Gupta, S.; Sud, M.; Byrnes, R. W.; Cotter, D.; Dinasarapu, A. R.; Maurya, M. R. *Chem. Rev.* **2011**, 111, 6452, DOI: 10.1021/cr200295k.
15. Dall'Armi, C.; Devereaux, K. A.; Di Paolo, G. *Curr. Biol.* **2013**, 23, 33, DOI: 10.1016/j.cub.2012.10.041.
16. Obeid, L. M.; Linardic, C. M.; Karolak, L. A.; Hannun, Y. A. *Science* **1993**, 259, 1769, DOI: 10.1126/science.8456305.
17. Lee, J. W.; Nishiumi, S.; Yoshida, M.; Fukusaki, E.; Bamba, T. *J. Chromatogr. A* **2013**, 1279, 98, DOI: 10.1016/j.chroma.2013.01.020.
18. Han, X.; Yang, K.; Gross, R. W. *Mass Spectrom. Rev.* **2012**, 31, 134, DOI: 10.1002/mas.20342.
19. Shanta, S. R.; Zhou, L.-H.; Park, Y. S.; Kim, Y. H.; Kim, Y.; Kim, K. P. *Anal. Chem.* **2011**, 83, 1252, DOI: 10.1021/ac1029659.
20. Mok, H. J.; Shin, H.; Lee, J. W.; Lee, G.-K.; Suh, C. S.; Kim, K. P.; Lim, H. J. *PLoS One* **2016**, 11, e0148577, DOI: 10.1371/journal.pone.0148577.

